INTERNATIONAL JOURNAL OF HYDROGEN ENERGY 41 (2016) 20185–20191

Available online at www.sciencedirect.com

ScienceDirect

journal homepage: www.elsevier.com/locate/he

Short Communication

Development of improved nickel catalysts for sorption enhanced CO_2 methanation

R. Delmelle [a,*], R.B. Duarte [a], T. Franken [a], D. Burnat [a], L. Holzer [b], A. Borgschulte [c], A. Heel [a]

[a] Institute of Materials and Process Engineering (IMPE), ZHAW – Zürcher Hochschule für Angewandte Wissenschaften, Winterthur, Switzerland
[b] Institute of Computational Physics (ICP), ZHAW – Zürcher Hochschule für Angewandte Wissenschaften, Winterthur, Switzerland
[c] Laboratory for Advanced Analytical Technologies, Empa – Swiss Federal Laboratories for Materials Science & Technology, Dübendorf, Switzerland

ARTICLE INFO

Article history:
Received 29 March 2016
Received in revised form
7 September 2016
Accepted 8 September 2016
Available online 29 September 2016

Keywords:
CO_2 methanation
Catalysis
Zeolites
Water sorption

ABSTRACT

Sorption enhanced CO_2 methanation is a complex process in which the key challenge lies in the combined optimization of the catalyst activity and water adsorption properties of the zeolite support. In the present work, improved nickel-based catalysts with an enhanced water uptake capacity were designed and catalytically investigated. Two different zeolite frameworks were considered as supports for nanostructured Ni, and studied with defined operation parameters. 5Ni/13X shows significantly increased, nearly three-fold higher, operation time in the sorption enhanced CO_2 methanation mode compared to the reference 5Ni/5A, likely due to its higher water sorption capacity. Both catalysts yield comparable CO_2 conversion in conventional CO_2 methanation (without water uptake). Regeneration of the catalysts performance is possible via a drying step between methanation cycles under both reducing and oxidizing atmospheres; however, operation time of 5Ni/13X increases further after drying under air.

Introduction

Methane production from waste carbon dioxide with renewable hydrogen can become of crucial significance for future energy turnaround strategy in countries like Switzerland or Germany, because it contributes to the reduction of CO_2 emissions. Such CO_2 emissions can be reused and even valorized by its chemical conversion with hydrogen produced from renewable excess energy [1]. Conventional methanation processes involve nanostructured active metals on various supports (e.g. SiO_2 [2], ZrO_2 [3], Al_2O_3 [4], carbon nanotubes [5]). Despite the existence of other elements at the research level, Ni remains the best choice for the active metal when considering activity, selectivity and price [6]. The efficiency of CO_2 methanation, also known as Sabatier reaction (1), is increased by the application of Le Châtelier's principle, via the in-situ removal of water from the reaction sites, causing an

* *Corresponding author.*
E-mail address: renaud.delmelle@zhaw.ch (R. Delmelle).
http://dx.doi.org/10.1016/j.ijhydene.2016.09.045

equilibrium shift: the so called sorption enhanced methanation process [7,8] (see Fig. 1). Additionally, high selectivity to CH_4 is desired, and therefore uptake of water already at the reaction centre is optimal.

$$CO_2 + 4H_2 \rightleftharpoons CH_4 + 2H_2O,\ \Delta H^0 = -165\ \text{kJ/mol}. \quad (1)$$

Zeolites are materials commonly used as adsorber material in industrial processes such as dehydration of ethanol and flue gas cleaning of exhaust air, but can also be used as catalyst support [9,10]. Zeolite LTX (13X) provides 9 Å pores, which allow an easy diffusion of molecules inside the zeolite channels, and high water sorption capacity (26 $g_{water}/kg_{zeolite}$ at 21 °C and 53% relative humidity (RH)) [11,12]. Zeolite LTA (5A) was previously tested by the authors [7,13,14] and proved itself efficient in the sorption enhanced CO_2 methanation, due to its relatively good water uptake capability (23 $g_{water}/kg_{zeolite}$ at 21 °C and 53% RH) and adequate pore size (5 Å), that allows accessibility of the molecules involved in the Sabatier reaction to the internal zeolite surfaces [7,14]. It is essential to understand how the properties of the zeolite support affect the catalytic reaction in order to design catalysts with an improved yield, extended operation time or fast kinetics for the sorption enhanced CO_2 methanation. For example, the role played by the heat of water sorption by the zeolite is omitted in Eq. (1). As water sorption is vital in this application, 13X was subjected as support for sorption catalyst and compared to the 5A reference.

Zeolites have limited water sorption capacity; consequently a regeneration step, i.e. drying of the catalyst bed with a dry gas is required, preferably at the same temperature level to avoid time consuming cooling and heating periods without operation [15]. Proper choice of the drying gas is a strategic key parameter: reducing environment yields higher reduction degree of the metallic active phase, which might result in higher catalytic activity [16]; however, a higher oxygen partial pressure obtained by an air stream allows cleaning of the catalyst surface from poisons present in CO_2 sources [17,18] or from coke, an intermediate species of the methanation reaction [19]. We elucidate the influence of the atmosphere used for the regeneration of the water saturated zeolite and of the zeolite support on the performance of nickel catalysts for sorption enhanced CO_2 methanation.

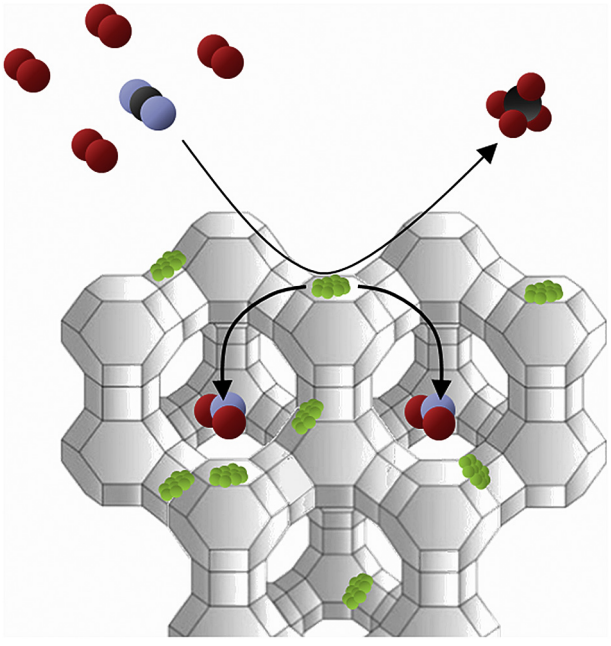

Fig. 1 – Molecular structure model of sorption enhanced CO_2 methanation over a nickel catalyst on zeolite. Red, blue, black and green spheres represent hydrogen, oxygen, carbon and nickel atoms, respectively. (For interpretation of the references to colour in this figure legend, the reader is referred to the web version of this article.)

Experimental

Nickel catalysts were supported on commercial zeolites LTA and LTX (beads, 2 mm, Zeochem) by a wet impregnation process from a solution of nickel nitrate hexahydrate ($Ni(NO_3)_2 \cdot 6H_2O$, Sigma Aldrich) in water. Zeolites were dried at 140 °C for 12 h before synthesis. The mixture of zeolite beads and Ni solution was stirred for 1 h at room temperature (RT) and subsequently the solvent was removed at 70 °C in a rotary evaporator. The samples were dried again for additional 12 h at 140 °C and then calcined at 500 °C in a muffle for 4 h to remove residual nitrate salts. Inductively Coupled Plasma Optical Emission Spectrometry (ICP–OES) measurements of the catalysts revealed that all samples contain about 4 wt.% nickel before calcination and 5 wt.% nickel after calcination, in agreement with the values calculated for the Ni supported zeolite with and without adsorbed solvent, respectively. The resulting samples are named 5Ni/5A and 5Ni/13X if prepared on LTA and LTX, respectively.

Catalytic screening of material systems for CO_2 methanation was performed in a tubular fixed-bed reactor with volume of 340 mL and an internal diameter of 32.8 mm coupled to a mass spectrometer (MS), model Pfeiffer OmniStar GSD 320 O1. The reactor contains a catalyst mass of 250 g. The reactions were carried out under atmospheric pressure. Samples were initially reduced for 1 h at 500 °C in 800 mL/min of a 1:1 molar ratio of H_2/Ar before reaction. After cooling to 300 °C under this reducing atmosphere, CO_2 methanation was performed with a GHSV (gas hourly space velocity = reactant gas flow rate per reactor volume) of 92 h^{-1} and reactant feed composition of CO_2 and H_2 with total flow of 520 mL/min and molar ratio 1:4.05 (5% excess of hydrogen to avoid coking). Argon was added at the reactor outlet as tracer prior to the MS for normalization of the MS signal. The activity and stability of the catalysts were tested at a reactor temperature of 300 °C according to the following sequence: (i) initially, the samples were subjected to CO_2 methanation up to the saturation of the zeolite support with water, identified by the breakthrough of water; (ii) the samples were then dried for 20 min with a flow of 800 mL/min of air or 1:1 molar ratio of H_2/Ar (zeolite drying time was prolonged to 40 min at specific tests to determine the influence of drying time in the subsequent test under sorption enhanced CO_2 methanation mode); (iii) the whole cycle procedure was then repeated six times. The amounts of H_2, CO, CO_2 and CH_4 were recorded by the MS as function of time. The flow rate was controlled by mass flow controllers (Bronkhorst,

FLOW-BUS). The outlet concentration was derived from a calibration line, assuming that the signal for CO_2 in the absence of the gas corresponded to full conversion, and that the signal without conversion was the flow rate set at the inlet. Conversion of CO_2 (X_{CO_2}) is defined as

$$X_{CO_2} = \frac{\Phi CO_{2,in} - \Phi CO_{2,out}}{\Phi CO_{2,in}} = 1 - \frac{\Phi CO_{2,out}}{\Phi CO_{2,in}}, \quad (2)$$

where $\Phi CO_{2,in}$ and $\Phi CO_{2,out}$ were the molar flow rates of CO_2 at the inlet and outlet of the reactor, respectively.

Metal particles were identified by scanning electron microscopy (SEM) and images were acquired with a FIB-SEM Helios Nanolab 600i (FEI). Good contrast settings were achieved with the so-called through-the-lens detector (TLD) at 2–3 kV accelerating voltage and low beam current (<100 pA). The phase content and crystal structure of powder specimens were analysed by X-ray diffraction (XRD) on a Bruker D8 Advance. Mean nickel crystallite sizes were determined by averaging the crystallite sizes calculated from the Ni (111), Ni (200) and Ni (220) reflections by the Scherrer equation. Peak broadening was determined by Rietveld refinement in the Topas software. Temperature programmed reduction experiments (TPR) were performed on a Quantachrome Autosorb iQ with an internal thermal conductivity detector (TCD). The samples were preoxidized in a flow of synthetic air at 500 °C for 2 h. Adsorbed oxygen was purged from the samples with N_2 at 500 °C for 30 min. After cooling down the samples in N_2-atmosphere the TPR was performed with a temperature ramping of 5 K/min up to 850 °C in a Flow ($\dot{V}$(gas) = 25 mL/min) of 5% H_2 in N_2.

Results and discussion

Fig. 2a and b shows representative SEM images of 5Ni/13X after reduction. The spherical spots correspond to nickel nanoparticles, while the typical fibrous and flake like large grey structures represent the zeolite 13X support. Nickel nanoparticles are homogeneously distributed throughout the zeolite support. Although a broad Ni particle size distribution (PSD) was observed, most particles are in the range 20–30 nm. As shown on Fig. 2c, XRD analysis of the reduced zeolites reveals the existence of mixed zeolite phases and metallic nickel. This is consistent to the different zeolite morphology which can be seen in the SEM images. Rietveld refinement was performed on the main Ni reflections from high-resolution acquisitions. Such calculations resulted in an average crystallite size of 33 ± 4 nm for 5Ni/13X and 22 ± 5 nm for 5Ni/5A, respectively, which is compatible with the observations from SEM analysis.

In order to understand the samples behaviour during reduction, TPR experiments were conducted with hydrogen as the reducing gas. Fig. 3 shows H_2-TPR experiments performed on both catalyst systems. On the one hand, Ni particles on zeolite 13X display a wide range of reduction temperatures, with several peaks indicative for oxide regions of different stabilities. On the other hand, Ni particles on zeolite 5A exhibit a very different TPR profile: most of the nickel oxide is reduced above 500 °C, as opposed to 5Ni/13X, which is already active at 300 °C. This result has important potential consequences on

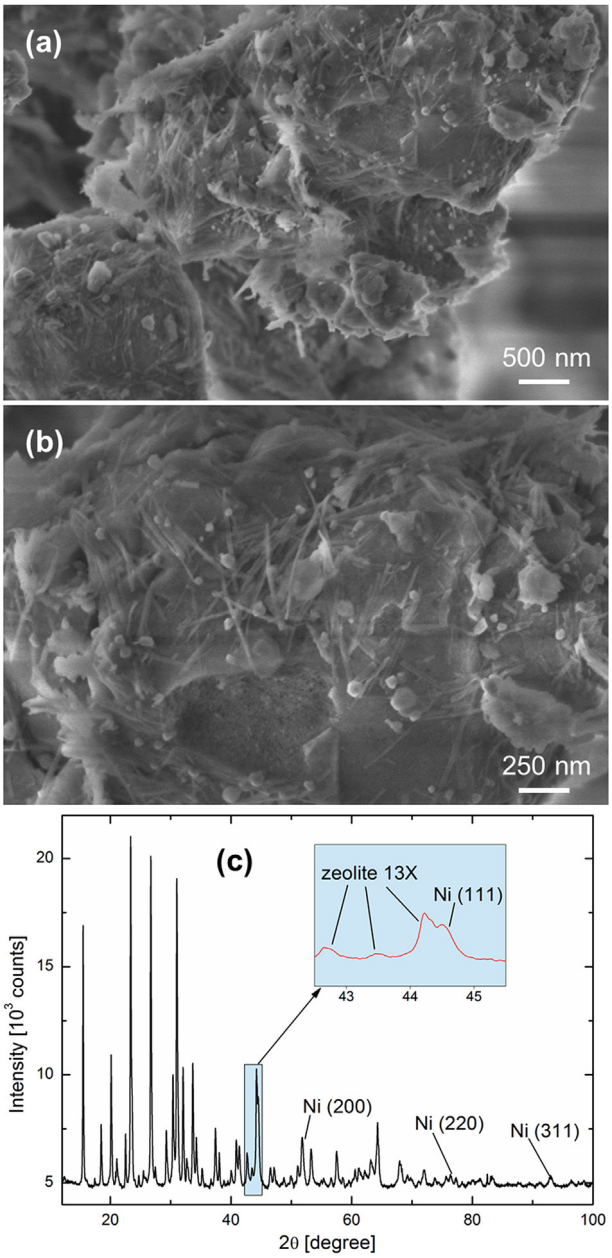

Fig. 2 – (a) and (b) Representative SEM images of 5Ni/13X after reduction. (c) XRD diffractogram of the same sample. Main reflections from Ni are shown, the other peaks correspond to zeolite 13X.

the choice of the catalyst/support couple, depending on the temperature of the application considered. In the case of sorption enhanced methanation, we showed that 300 °C is the optimal operation temperature [13]. If the catalyst regeneration can take place at this temperature, the CO_2 methanation efficiency according to Eq. (1) is increased. This is of great advantage and in favour of 13X as support.

Fig. 4a shows the alternated cyclic CO_2 methanation and drying treatment applied to the catalysts at an operation temperature of 300 °C in the reactor. Cyclic tests were initiated with CO_2 methanation after pre-reduction of the catalysts at

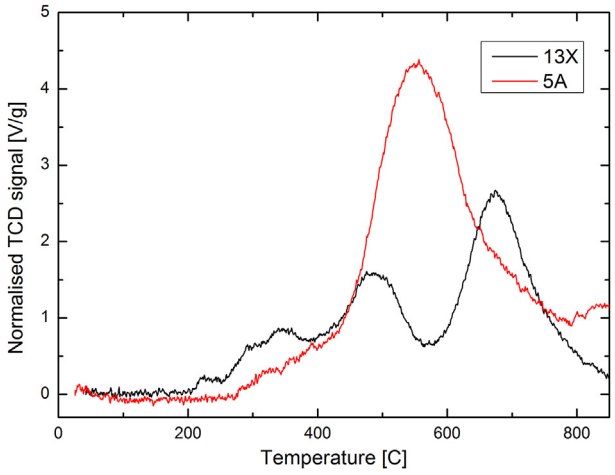

Fig. 3 – H_2-TPR profiles of 5Ni/13X and 5Ni/5A.

500 °C. The measured normalized time of operation (NTO) under sorption enhanced CO_2 methanation mode of 5Ni/5A and 5Ni/13X catalysts is given as a function of the number of cycles in Fig. 4b. The NTO is calculated as

$$NTO = t \cdot \frac{F}{V}, \quad (3)$$

where t is the time of operation under sorption enhanced CO_2 methanation mode, F is the flow rate and V is the reactor volume. The catalysts are subjected to six cycles, each consisting of a reaction and a regeneration step to determine catalyst stability. The local temperature in the reactor rises about 30 °C during the catalytic tests due to the exothermicity of both, the CO_2 methanation and the water adsorption on zeolites [8]. This is in accordance to our previous results [7,13].

Both, 5Ni/5A and 5Ni/13X yielded full CO_2 conversion and reached a dry product gas flow with 100% selectivity to CH_4. However, the 5Ni/13X composite even allowed a substantial extension of the operation time for the CO_2 methanation in the sorption enhanced mode if compared to 5Ni/5A.

Additionally, an intermediate drying step under air led to a further 26% longer NTO in the sorption enhanced methanation mode for 5Ni/13X, in comparison to a drying step under reducing environment. In contrast, for 5Ni/5A the NTO is almost identical for reducing and oxidizing drying conditions. It has to be mentioned, that both catalysts showed a substantially extended NTO in the very first cycle: 121% and 234% longer than for the average NTO in the following CO_2

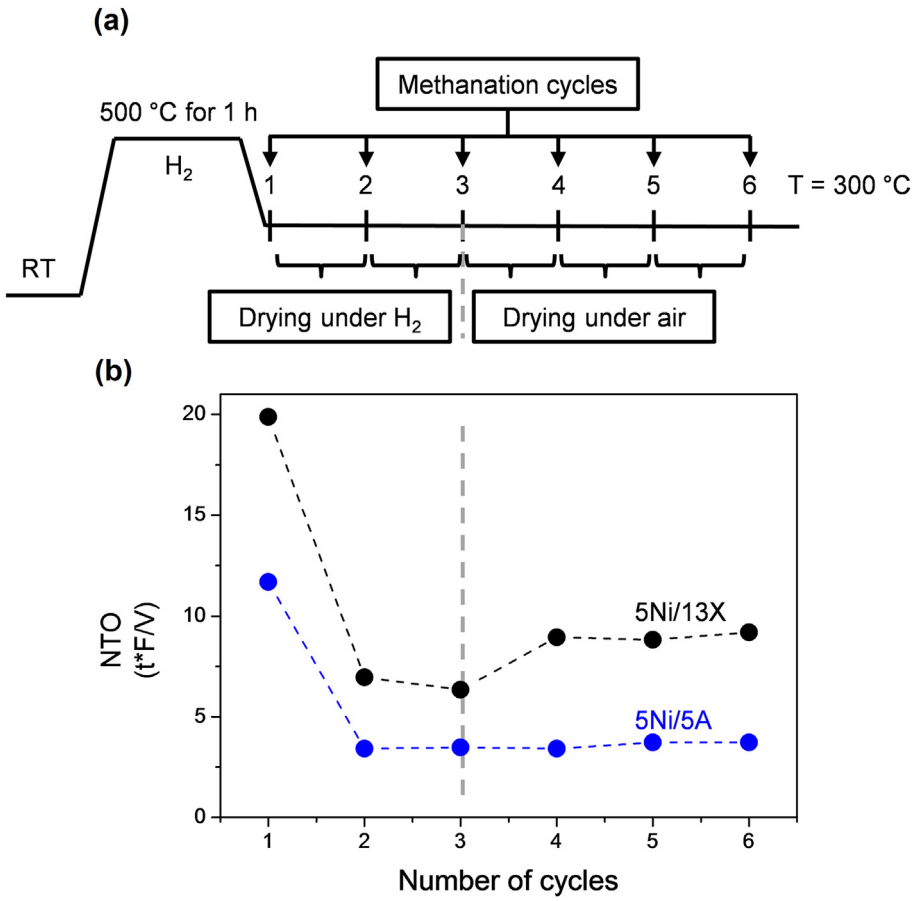

Fig. 4 – (a) Treatment related to alternated cyclic CO_2 methanation and drying treatment applied to the catalysts at 300 °C reactor temperature and (b) NTO of sorption enhanced CO_2 methanation during cyclic tests with 5Ni/5A and 5Ni/13X (the black, blue and grey dashed lines are only a guide to the eye). Between cycles 5 and 6, the drying step was carried out for twice as long, i.e. 40 min. (For interpretation of the references to colour in this figure legend, the reader is referred to the web version of this article.)

methanation tests in sorption enhanced mode for 5Ni/13X and 5Ni/5A, respectively. As shown in Fig. 3, this is likely due to the pre-treatment under H_2/Ar at 500 °C, causing a higher reduced nickel phase (c.f. Ref. [20]). That the effect of reducing the catalyst at 500 °C is twice more pronounced for 5Ni/5A can be explained by the TPR data of Fig. 3, indeed showing that reducing 5Ni/5A at 300 °C will be significantly less effective than 5Ni/13X. However, in fair agreement with the data for the following cycles the activity of the catalysts can be described as stable. 5Ni/5A has an average NTO of 3.5 while 5Ni/13X showed a NTO of 9 when dried under oxidizing environment, a value nearly three-fold higher than for 5Ni/5A. The improved performance of 5Ni/13X in terms of operation time under sorption enhanced conditions can be explained by its higher water sorption capacity, especially when considering the high temperature of the sorption enhanced methanation process. Indeed, although the room temperature water sorption capacity of zeolite 13X is only 13% higher than 5A (see introduction), this difference increases with temperature. Extrapolating the model from Wang and LeVan [21] to 300 °C brings it to 135% (2.9 $g_{water}/kg_{zeolite}$ for 5A and 6.7 $g_{water}/kg_{zeolite}$ for 13X). Although these values are small compared to the room temperature sorption capacities, they turn out to have considerable effect on the methanation performance.

The restoration of the catalytic properties reached after drying is due to the regeneration of the zeolite support, namely the renewal of its water sorption capacity. A straight correlation between nickel dispersion and catalyst performance is observed for CO_2 methanation according to literature [22]. Re-dispersion of the nickel metallic phase can take place due to metal-support interaction during drying under the influence of both oxidizing and reducing atmospheres [23,24], which might also result in the observed stability of these samples during the cycling between the sorption enhanced methanation mode and the drying mode.

5Ni/5A could be dried under H_2/Ar or air yielding approximately the same NTO for sorption enhanced CO_2 methanation. As previously mentioned, drying 5Ni/13X under air improves the NTO compared to a drying cycle under H_2/Ar. Oxygen and nitrogen molecules have sizes and weights that are comparable to the water molecule (i.e. on the same order of magnitude, as opposed to hydrogen). Collisions between these gas species are energetically more effective. Therefore, it is reasonable to assume that hydrogen does not carry out the water from the zeolite beads with the same efficiency as air. Additionally, hydrogen can be chemisorbed in nickel impregnated zeolites [14]. The difference in drying with air or hydrogen is pronounced only for 5Ni/13X probably due to the bigger pores of this support, which allows easier diffusion and release of the air and water molecules. In the drying step, kinetic diameters of the molecules involved reach 3.6 Å for nitrogen and 3.5 Å for oxygen, respectively [25]. Although this is small enough to enter the 5 Å pores of the 5A structure, it is clear that the 9 Å pores of the 13X structure allow for a faster transport of these molecules. However, it should be noted that the catalyst could be regenerated after drying under both conditions, giving the same NTO as in the previous cycle. Under oxidative conditions cleaning of the catalyst surface by oxidation of catalyst poisons would be feasible [26], which is a desired asset for real applications: on one hand there is coke deposition, which is a common source of deactivation [27]. On the other hand CO_2 sources like biogas plants or cement clinker plants normally contain sulphur compounds, which can even lead to an irreversible catalyst poisoning [17].

It is worth to mention here, that no change in performance is observed when the time for the drying procedure is doubled (between cycles 5 and 6). Under the conditions applied in this work, maximum water sorption capacity of the zeolite is achieved already after 20 min under dry flow; longer drying periods do not cause any improvement.

Over both samples 100% selectivity to CH_4 is obtained during sorption enhanced CO_2 methanation (MS profile not shown, [7,13,14]). The authors observed that the selectivity for CH_4 is greatly enhanced if the pore size of the support is equal or larger than 5 Å: the pores of the 5A zeolites are large enough to accept the reactants and release the products [14]. However, as mentioned above, desorption from the catalyst might be hindered by pore diffusion limitations. The faster transport of air and water through the 5Ni/13X structure is crucial for the drying process.

Fig. 5 shows the CO_2 conversion rate of 5Ni/5A and 5Ni/13X catalysts during conventional CO_2 methanation, i.e. after saturation of the zeolite with water is reached and the sorption enhanced mode of the zeolite is eliminated. The average conversion of CO_2 at 300 °C is 78.8% for both, 5Ni/5A and 5Ni/13X catalysts. Zeolite 13X has a higher Si/Al ratio and therefore lower acidity than the zeolite 5A. The acidity of the support can be an important parameter, which affects the catalytic performance and product selectivity of a reaction [28]. However, the CO_2 conversion levels are rather similar for the different supports when the water sorption capacity of the support is removed, pointing to a sole performance dependence on the metallic nickel phase. Andersson et al. [19] proved by density functional theory (DFT) calculations that the methanation reaction is structure sensitive and therefore depends on the catalytic active metal particle shape and size.

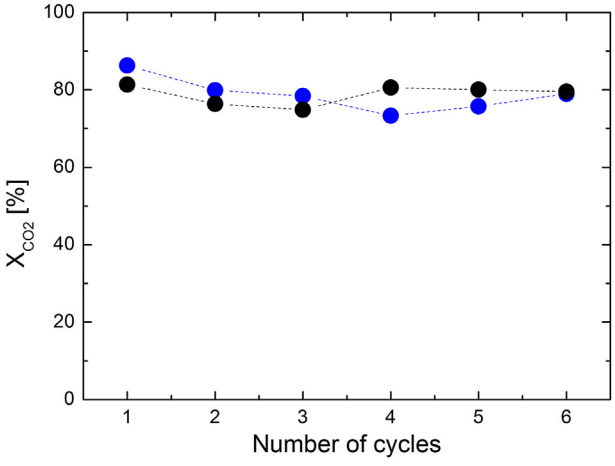

Fig. 5 – CO_2 conversion under conventional CO_2 methanation mode over 5Ni/5A (blue) and 5Ni/13X (black) at 300 °C. (For interpretation of the references to colour in this figure legend, the reader is referred to the web version of this article.)

Independent of the zeolite support, the good stability of the catalyst performance shown in Fig. 5 is an encouraging sign for potential applications. Regarding such applications, the authors previously showed that the temperature of 300 °C is a good compromise between water sorption capacity and catalytic activity [13]. More generally, the technical requirements of a given application should be put into perspective with this temperature optimum, which may change from one material to another.

Conclusions

Nickel catalysts supported on zeolites yield pure CH_4 during CO_2 methanation, up to the saturation of the zeolite support with water. This is the so-called sorption enhanced CO_2 methanation mode. The performance of the catalysts can be restored after drying under reducing or oxidizing environment.

When pre-dried under oxidizing atmosphere, 5Ni/13X catalyst showed a substantially improved performance and can be operated for nearly threefold longer time than 5Ni/5A in the sorption enhanced CO_2 methanation mode. The larger pores of the 5Ni/13X structure allow for better air and water transport, and therefore more efficient catalyst regeneration in oxidizing conditions. The authors are especially interested in using an oxidizing environment for the regeneration of the catalysts because such condition is particularly needed in real applications to counteract catalyst deactivation due to poisoning by coke and/or sulphur.

Acknowledgments

The authors are grateful for the financial support provided by the Bundesamt für Energie (SFOE) and the Swiss Gas Industry (FOGA) through the SMARTCAT project (grant number SI/501130-01) and by the Swiss National Science Foundation (SNSF, NRP70). We warmly thank Nicholas Stadie for discussion on the high temperature water sorption capacities.

REFERENCES

[1] Gotz M, Lefebvre J, Mors F, Koch AM, Graf F, Bajohr S, et al. Renewable Power-to-Gas: a technological and economic review. Renew Energ 2016;85:1371–90.
[2] Yan XL, Liu Y, Zhao BR, Wang Z, Wang Y, Liu CJ. Methanation over Ni/SiO_2: effect of the catalyst preparation methodologies. Int J Hydrogen Energy 2013;38:2283–91.
[3] da Silva DCD, Letichevsky S, Borges LEP, Appel LG. The Ni/ZrO_2 catalyst and the methanation of CO and CO_2. Int J Hydrogen Energy 2012;37:8923–8.
[4] Garbarino G, Riani P, Magistri L, Busca G. A study of the methanation of carbon dioxide on Ni/Al_2O_3 catalysts at atmospheric pressure. Int J Hydrogen Energy 2014;39:11557–65.
[5] Wang W, Chu W, Wang N, Yang W, Jiang CF. Mesoporous nickel catalyst supported on multi-walled carbon nanotubes for carbon dioxide methanation. Int J Hydrogen Energy 2016;41:967–75.
[6] Rönsch S, Schneider J, Mattischke S, Schlüter M, Götz M, Lefebvre J, et al. Review on methanation – from fundamentals to current projects. Fuel 2016;166:276–96.
[7] Borgschulte A, Gallandat N, Probst B, Suter R, Callini E, Ferri D, et al. Sorption enhanced CO_2 methanation. Phys Chem Chem Phys 2013;15:9620–5.
[8] Walspurger S, Elzinga GD, Dijkstra JW, Saric M, Haije WG. Sorption enhanced methanation for substitute natural gas production: experimental results and thermodynamic considerations. Chem Eng J 2014;242:379–86.
[9] Boudart M. Catalysis by supported metals. Adv Catal 1969;20:153.
[10] Suzuki M, Tsutsumi K, Takahashi H. Characterization and catalytic activity of nickel-zeolite catalysts. IV. Effects of support on dispersion of nickel and catalytic activity. Zeolites 1982;2:193–9.
[11] Janchen J, Stach H. Adsorption properties of porous materials for solar thermal energy storage and heat pump applications. Energy Proced 2012;30:289–93.
[12] Tatsidjodoung P, Le Pierrès N, Heintz J, Lagre D, Luo L, Durier F. Experimental and numerical investigations of a zeolite 13X/water reactor for solar heat storage in buildings. Energy Convers Manag 2016;108:488–500.
[13] Borgschulte A, Delmelle R, Duarte RB, Heel A, Boillat P, Lehmann E. Water distribution in a sorption enhanced methanation reactor by time resolved neutron imaging. Phys Chem Chem Phys 2016;18:17217–23.
[14] Borgschulte A, Callini E, Stadie N, Arroyo Y, Rossell MD, Erni R, et al. Manipulating the reaction path of the CO_2 hydrogenation reaction in molecular sieves. Catal Sci Technol 2015;5:4613–21.
[15] Jenkins SA, Waszkiewicz S, Quarini GL, Tierney MJ. Drying saturated zeolite pellets to assess fluidised bed performance. Appl Therm Eng 2002;22:861–71.
[16] Ligthart DAJM, van Santen RA, Hensen EJM. Influence of particle size on the activity and stability in steam methane reforming of supported Rh nanoparticles. J Catal 2011;280:206–20.
[17] Ashrafi M, Pfeifer C, Proll T, Hofbauer H. Experimental study of model biogas catalytic steam reforming: 2. Impact of sulfur on the deactivation and regeneration of Ni-Based catalysts. Energ Fuel 2008;22:4190–5.
[18] Hulteberg C. Sulphur-tolerant catalysts in small-scale hydrogen production, a review. Int J Hydrogen Energy 2012;37:3978–92.
[19] Andersson MP, Abild-Pedersen E, Remediakis IN, Bligaard T, Jones G, Engbwk J, et al. Structure sensitivity of the methanation reaction: H_2-induced CO dissociation on nickel surfaces. J Catal 2008;255:6–19.
[20] Tan MW, Wang XG, Wang XX, Zou XJ, Ding WZ, Lu XG. Influence of calcination temperature on textural and structural properties, reducibility, and catalytic behavior of mesoporous gamma-alumina-supported Ni-Mg oxides by one-pot template-free route. J Catal 2015;329:151–66.
[21] Wang Y, LeVan MD. Adsorption equilibrium of carbon dioxide and water vapor on zeolites 5A and 13X and Silica Gel: pure components. J Chem Eng Data 2009;54:2839–44.
[22] Van Santen RA. Complementary structure sensitive and insensitive catalytic relationships. Acc Chem Res 2009;42:57–66.
[23] Davidova NP, Valcheva ML, Shopov DM. Study of the dispersion of zeolite supported nickel in dependence on the zeolite type and the reaction medium. Stud Surf Sci Catal 1984;18:353–60.
[24] Ueckert T, Lamber R, Jaeger NI, Schubert U. Strong metal support interactions in a Ni/SiO_2 catalyst prepared via sol-gel synthesis. Appl Catal A-Gen 1997;155:75–85.

[25] Mehio N, Dai S, Jiang D. Quantum mechanical basis for kinetic diameters of small gaseous molecules. J Phys Chem A 2014;118:1150–4.
[26] Alstrup I, Rostrup-Nielsen JR, Røen S. High temperature hydrogen sulfide chemisorption on nickel catalysts. Appl Catal 1981;1:30–314.
[27] Goralski J, Grams J, Paryjczak T, Rzeznicka I. Investigation of the coke deposit on Ni-Al_2O_3 and Co-Al_2O_3 catalysts. Carbon 2002;40:2025–8.
[28] Corma A. Inorganic solid acids and their use in acid-catalyzed hydrocarbon reactions. Chem Rev 1995;95:559–61.